Bulletin of Glaciological Research 20 (2003) 49–55

Field-performance tests of a portable low-frequency ice-penetrating radar and a ground-penetrating radar at Athabasca Glacier, Canadian Rockies

Kenichi MATSUOKA*, Tatsuto AOKI, Tatsuya YAMAMOTO and Renji NARUSE**
Institute of Low Temperature Science, Hokkaido University, Sapporo 060-0819 Japan.

(Received September 18, 2002; Revised manuscript received November 19, 2002)

Abstract

Field tests of a novel portable low-frequency ice-penetrating radar (IPR) and a commercial ground-penetrating radar (GPR) were performed in September 2001 at Athabasca Glacier in Jasper National Park, Alberta, Canada. We measured about 110 m of ice thickness with the IPR at a point in the middle reaches of the glacier and acquired experiences for future practical usages. The GPR detected the bedrock reflection continuously beneath <15-m-thick ice at the glacier terminus and pseudo received power from the englacial and subglacial reflectors were calculated in this range. On the lateral ice-cored moraine, we traced with the GPR along two lines, where debris thickness changed from zero to 55 cm. The interface between debris and ice was clearly recognized when debris had sandy-silt matrix, whereas it was not identified when debris were composed of cobbles. It is probably due to large scattering of radio wave from the large gravels. Preliminary interpretations on the velocity and attenuation within ice and debris were also discussed.

1. Introduction

Mountain glaciers play important roles on water and energy cycles in the earth environments. Since the response time of mountain glaciers to climate change is at least two orders less than that of polar ice sheets, monitoring of glacier volume is required from the point of view of global sea-level rise (IAHS/UNESCO, 1998; Meier, 1984). Large amounts of melt cause to form subglacial, englacial, and supraglacial water channels in summer. Water-induced complex features make us difficult to understand mechanisms of glacier variations. Nevertheless, real glacier features must be known before modeling the glaciers to predict their future variations. Besides glaciers, such a periglacial landform as an ice-cored moraine stores significant amount of ice. Debris thickness of the moraine is critical for the heat balance of underlying ice. However, there are no well-developed practical methods to know the spatial variations of the thickness.

Radio-wave remote sensing is one of the most powerful methods to achieve these requirements. Since there are significant contrasts of dielectric properties among ice, water, air, and rock/sediments, we can visualize subsurface structures with radars (*e.g.* Bogorodskiy *et al.*, 1985; Plewes and Hubbard, 2001). However, current instruments are not sufficient to investigate glacier and periglacial environments; we need an advanced system which is low-power consumption, light, and user-friendly. Moreover, knowledge of performance and limitation of radar survey are still limited.

Based on previous ice-penetrating radars (hereafter, IPR), we started to develop a less-weight, less-power-consumption, more-user-friendly IPR since 2000. The IPR is a part of the novel glacier profiler system, with which we can know the elevations of glacier and bedrock surfaces. Bedrock elevations are essential to numerical glacier models.

In addition to the above IPR, we have carried out basic experiments since 2000 winter to apply a commercial ground-penetrating radar (hereafter, GPR) for glaciological studies. As a consequence, we carried out field tests of the glacier profiler and the GPR at Athabasca Glacier in Jasper National Park, Alberta, Canada from September 10 to 22, 2001, to know their performance and limitation, and to acquire experiences of these operations. This report is an overview of the field activities, and presents preliminary results and their interpretations.

*Present affiliation: Research Institute for Humanity and Nature, Kyoto 602-0878 Japan.
**Present affiliation: Department of Geography, Kanazawa University, Kanazawa 920-1192 Japan.

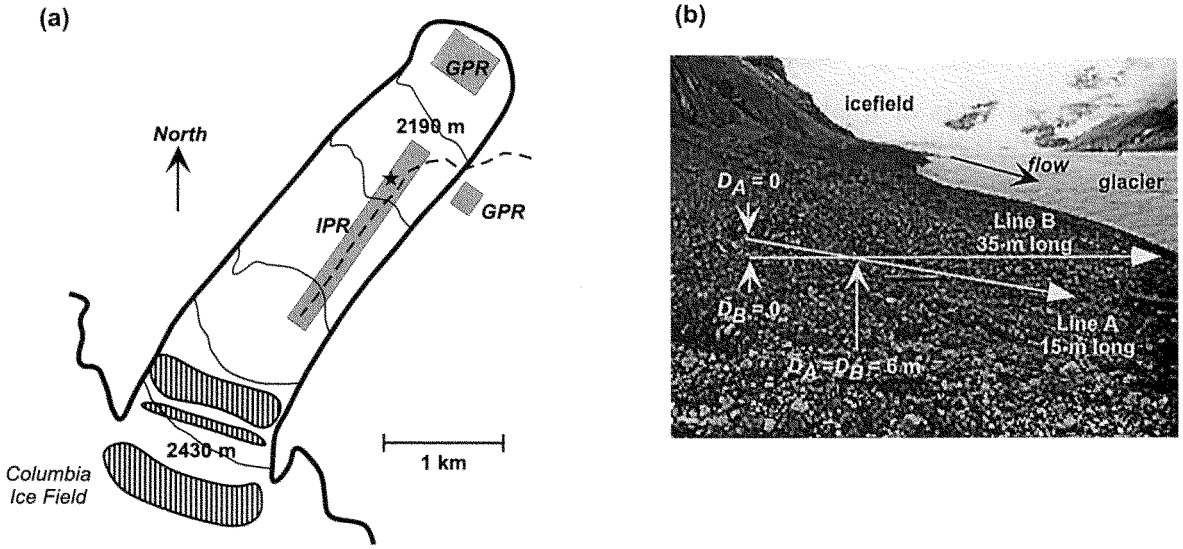

Fig. 1. Athabasca Glacier. (a) Geographical map. Thick line represents the glacier boundary, and hatched areas indicate three icefalls. Counter-line intervals are 200 feet (61 m). A dotted line shows the snocoach trail from the parking area on the lateral moraine to the turnaround in the middle of the glacier. Shaded areas are test sites for ice-penetrating radar (IPR) and for ground-penetrating radar (GPR). A star shows the site where we obtained ice thickness. (b) GPR survey lines on the right marginal lateral moraine. D_A and D_B show locations (distances) along these two lines.

2. Geographical setting

2.1. Athabasca Glacier

Athabasca Glacier is a northeastward tongue of the Columbia Icefield (Fig. 1a). Following three steep icefalls, the relatively gentle glacier spreads 1 km wide and 3.5 km long between 2000 m a.s.l. (the terminus) and 2400 m a.s.l. (the lowest icefall). Ice thickness over the glacier was well investigated by Trombley (1986). Ice becomes thicker with the distance upglacier, and reaches the maximum thickness larger than 320 m. An analysis of aerial or terrestrial photographs showed that the glacier lost 2.344×10^8 m^3 of volume and downwasted significantly for the period 1919-1979 (Reynolds and Young, 1997). The glacier underwent a rapid recession; 1.2 km during 1922/1980 (Rutter and Luckman, 1987). In addition to the recent glacier retreat, Athabasca Glacier has retreated largely since the Little Ice Age (Rutter and Luckman, 1987). As a result, we can see well-developed lateral and terminal moraines.

We performed the field tests from September 10 to 22, 2002. This period was in the late melting season, or a transition between the melting season and the early winter. We found many supraglacial and englacial water channels, and moulins. These conditions are typical for mountain glaciers in the ablation season. Then, these field tests in this period provide useful information for the future practical usage of the IPR and GPR.

2.2. Test sites

2.2.1. On the glacier

The novel glacier profiler system with the IPR was tested on the snocoach (special bus for tourists) trail and the turnaround in the middle reaches of the glacier (Fig. 1a), since they were maintained daily by Brewster Company and hence kept smooth. In addition to the current trail, the former trail near the current one was also used. Previous studies showed that ice thicknesses around the turnaround and previous/current snocoach trail nearby the lateral moraine are about 300 m and 100 m, respectively (Trombley, 1986).

The GPR was tested at the glacier terminus, tracing along a longitudinal line from the glacier terminus (Fig. 1a). In addition, we carried out detailed investigations where foliation and moulins existed, of which results will be presented elsewhere.

2.2.2. On the ice-cored moraine

The GPR was tested also on the ice-cored lateral moraine adjoining the glacier (Fig. 1b). The moraine is characterized with steep slope on the glacier side and older moraine sequences on the other side. The top area is flat with small (<about 0.3 m) undulations. Two study lines were set as shown in Fig. 1b; one was 15 m long on the top area (line A), and the other was 35 m long across the moraine (line B). Debris-surface conditions along the lines A and B are uniform and change, respectively. Debris stratigraphies were studied by pit work at three sites, and grain-size distribution and water content for upper and lower parts of the middle layer were measured at a site along the line B (Fig. 2). There are relatively large gravels and small matrix on the side slope ($D_B > 8$ m) and the top area ($D_B < 8$ m), respectively. Since line A is located on the top gentle area, we can consider that debris matrix

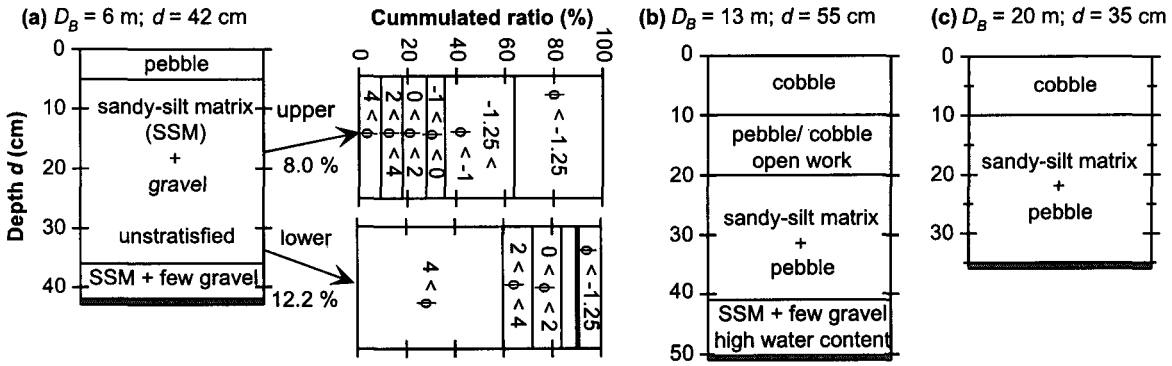

Fig. 2. Debris stratigraphy at (a) $D_B=6$ m, (b) $D_B=13$ m, and (c) $D_B=20$ m along the line B. The depth (d) at each site is given at the top of each panel. Gray bands represent top surfaces of the core ice. Sites (a) and (b) are on the top flat area of the lateral moraine, whereas the site (c) is on the steep slope. SSM represents sandy-silt matrix. Note that water contents and grain-size distribution represent with weight percent and phai scale, respectively.

along the line A is uniform with the sandy-silt matrix as observed at $D_A=D_B=6$ m. Since it was difficult to pull the GPR on the gravel surface, we carried the GPR about 5 cm above the debris.

3. Tested instruments

3.1. *Glacier profiler system with portable low-frequency ice-penetrating radar*

Our novel glacier profiler is composed of the originally-designed IPR, a Global Positioning System receiver (GPSR), a barometer and an odometer (Fig. 3a). All components are connected to the controller (CT), which is basically composed of conventional parts of personal computers. However, the CT has a high brightness display and is waterproofed. The total weight of this system is 10 kg including batteries. Total power consumption is 24 W (display: on) and 19 W (display: off).

The IPR is composed of a transmitter (Tx), a receiver (Rx), and two sets (transmitting and receiving) of resistivity-loaded half-length dipole antennas (ANTs). We used 5-MHz antennas for this field test, but we can change the frequency. The ANTs are connected to the Tx or Rx directly. Not electrical but optical-fiber cables connect Tx and Rx to CT, to prevent interference between such communication lines (30 m in length) and ANTs (10 m in length). To avoid cables harden under low temperatures, we carried out mechanical tests in cold rooms in advance and

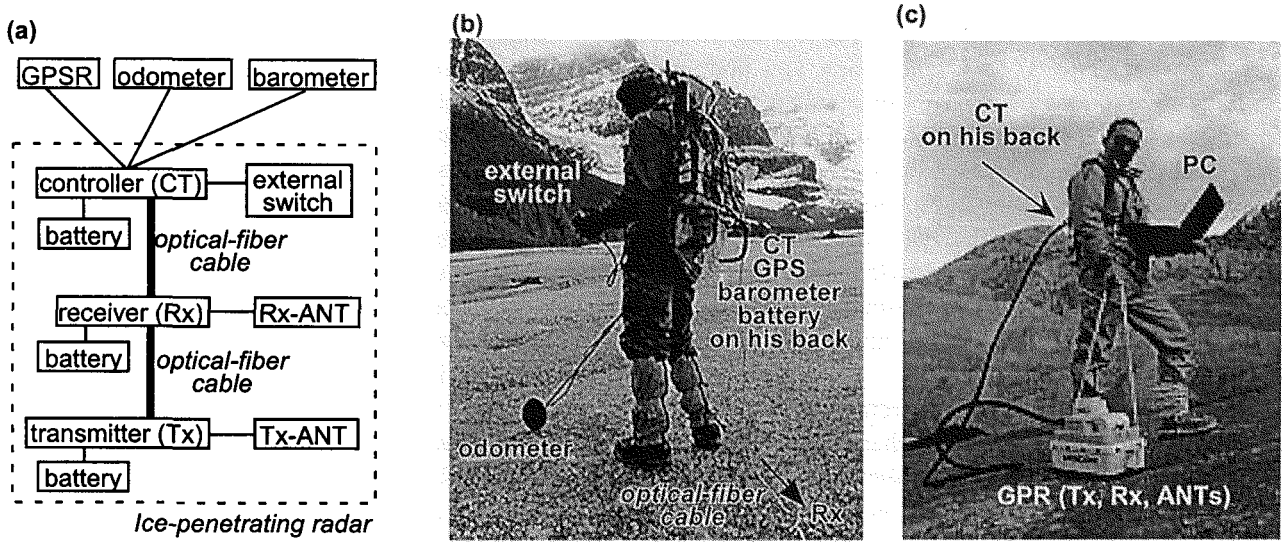

Fig. 3. Tested instruments. (a) Block diagram of the glacier profiler system. Thick and thin lines show optical-fiber and electrical cables, respectively. Length of electrical cables is less than 2 m. Antennas (ANTs) are directly connected to the Tx and Rx. (b) Photo of the glacier profiler system. Although there are both external switch and odometer, each of them can be used for the triggering at a time. (c) Photo of the ground-penetrating radar (GPR). Package on the glacier contains antennas, Rx and Tx. The CT triggers Tx and Rx according to given observation parameters from the PC. Also, the PC displays quick-look data.

chose flexible rubber-covered cables for ANTs and communication lines.

The IPR works as the following architecture. A 900 V pulse is generated within the Tx according to a trigger from the CT and sent to the transmitting ANT. Time series of the received voltage are digitized and stacked in the Rx. After averaging the stacked waveforms, an averaged datum is sent finally to the CT. The timing of data acquisition is provided automatically according to a given time or distance interval, or manually with an external button. Although duration to acquire one datum depends on flexible parameters (time window width and stacking number), it requires us between 10 and 30 seconds for the typical cases. In addition, auto-transmission mode is equipped for checking the instrument. Pushing an internal switch, Tx sends the pulse continuously and we can observe waveform with an oscilloscope connected Tx directly or connected Rx antenna (that is checking transmitting voltage and total performance of Tx and antennas, respectively).

The GPSR and the barometer provide horizontal positions and height differences within errors of 15 m and 0.2 hPa, which is equivalent to the 2-m-height change, respectively. Therefore, combining with another barometer at a fixed site (*e.g.* camp site) to know time series of air pressure due to the weather change, we can achieve elevation changes of glacier and bedrock surfaces with this glacier profiler system. Time, horizontal position, and air pressure are attached to each IPR datum. Data are stored in a removal hard disk (flush card) in the CT.

Continuous observations with this glacier profiler system can be carried out by two (minimum) or three (recommended) people. As shown in Fig. 3b, the first person carries the CT on his/her back and pulls a climbing rope (diameter 3 mm). Communication lines and ANTs are tied with the rope to prevent significant tension applied to these cables. The second person pulls the Rx, and the third person pulls the Tx (optional; it can be pulled by the second person with the climbing rope, if the glacier surface is gentle). The distance between these people is around 13 m, and the transmitting and receiving ANTs are in the collinear relation.

In addition to traverse measurements, this system can be used for measurements with common-midpoint method, which is usually used to know water contents (Macheret *et al.*, 1993). The common-midpoint method requires multiple measurements at a point with different antenna separations between several tens meters and one hundred meters. For this measurement, we can replace 30-m optical fiber cable with 100-m one. If we use optical fiber cable with different length, propagation time of a trigger between Rx and Tx will change. To calibrate this time lag, we have to identify length of the cable with CT.

3.2. Ground-penetrating radar

We used Ramac ground-penetrating radar, which is a manufacture of MALÅ GeoScience, Sweden (Fig. 3c). It was applied for glacier studies (Moore *et al.*, 1999). MALÅ GeoScience provides antenna units of several frequencies, and we choose 800 MHz antenna unit. Ramac GPR requires a laptop personal computer (PC). We used one for heavy-outdoor use (Panasonic, Toughbook series), which has high-brightness and touch-panel display, and is semi-water proof. Such flexible parameters as time window width and sampling rate are set with a software on the PC. Including this PC and batteries, total weight and power consumption are 17 kg and 70 W, respectively.

GPR observations can be carried out by one person (Fig. 3c). He/she carries a controller on his/her back, operates the PC, and pulls a package which includes Tx, Rx, and ANTs. Nevertheless, operations with two people are much more effective.

4. Results and interpretations

We tested the glacier profiler system and the GPR for five and six days, respectively. The tests had two parts. The first one is to check their appropriate work under severe conditions and to acquire experiences for the future usage. The second one is to know their potential performance. The target of the glacier profiler system is ice-thickness profiles over a glacier, and that of GPR is ice thickness near the glacier terminus and debris thickness of the ice-cored moraines.

4.1. Operation tests

Glacier profiler worked well in general, even at low temperatures and on the wet surface. Moreover, the high-brightness display enabled us to watch it clearly even under sunshine. However, data transmission from Rx to CT was sometimes broken. Post laboratory tests in a cold room (-15 °C) showed that it was due to temperature dependence of a communication module in the CT. Except this point, other instruments worked well. We confirmed that the output voltage of the Tx was the same as the designed one (900 V). This indicates that impedance of the transmitting ANT on wet ice was about 50 ohm, which was the designed value for Tx-output impedance.

The GPR worked well even at low temperatures. Also, the heavy-use PC enabled us to operate it without significant stress. However, batteries of the GPR were not sufficient for full-day use. We could operate it only one or two hours, even if we charged it fully. To overcome this point, high-density compact batteries for home-use video cameras (SONY Handycom, for example) will be applicable. The voltage of the battery (Lithium ion) matches to that of the Ramac (7.2 V).

4.2. Performance tests

4.2.1. Ice-penetrating radar for ice thickness measurements

Since communications between Rx and CT of the glacier profiler system were sometimes broken, we used auto-transmission mode of the Tx and connected the receiving ANT to the oscilloscope directly to observe the received waveform. Antennas were set parallel to each other and perpendicular to ice flow direction (as it usually uses for the common-midpoint method).

Figure 4 shows time series of received voltage at the site shown in Fig. 1a. A large voltage change was found at the delay time of 1.28 μs. If we used 169 m μs^{-1} for a wave propagation speed within the pure ice at low temperatures (Fujita *et al.*, 2000), it corresponded to 105 m in depth. We considered that this voltage change was reflected from subglacial surface beneath the observation site based on the following two facts. First, polarity is opposite to the air wave. In general, since permittivity of rock (and water) is larger than that of ice, polarity of received voltage from subglacial surface is opposite to the air wave. Next, it is the final large change of voltage. Dipole antennas radiate radio wave not only into the ice but also other directions. In case of valley glaciers, we can receive reflections from mountains around the glacier. However, since we set antennas perpendicular to ice flow, radiation components of radio wave in the direction of lateral mountains is significantly smaller than that of ice. Moreover, the previous study showed that bedrock topography around this area is gentle and we can expect that it is infrequent to observe side-looking reflections in prior to the beneath reflection.

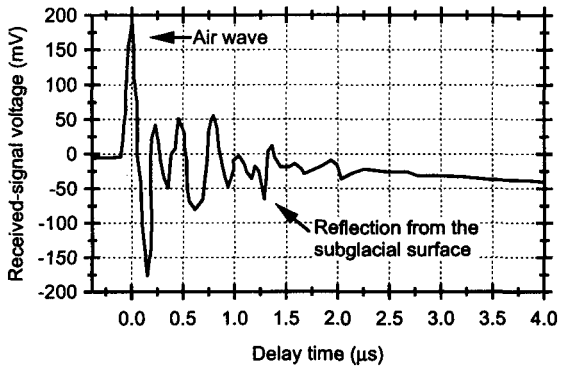

Fig. 4. Time series of received voltage at the site shown with the star in Fig. 1a.

Water within the ice affects the propagation speed (Macheret *et al.*, 1993). If we assume that there is no interaction between ice and water and permittivity of a mixture of ice and water is calculated by Looyenga equation (Paren and Robin, 1975), we can evaluate the effect of water on the propagation speed. A simple calculation showed that the speed decreases about 5 m μs^{-1}, as the water content increases 1%. If we assume the water content as 3%, the depth is 95 m. Nevertheless, estimated ice thickness nearly matched the ice-thickness map of Trombley (1986). As a result, although our novel glacier profiler system needs improvements especially on the communication components of Rx and CT, its design and basic performance achieved our requirements.

4.2.2. Ground-penetrating radar for ice thickness measurements

A pseudo-cross section (so called Z-scope) of the glacier terminus obtained with the GPR is shown in Fig. 5. The delay time was converted to depth with a propagation speed of 169 m μs^{-1}. Slope of the glacier surface was constant at 13°, and the slope of the reflection surface was about 14°. This agreement suggested that the subglacial topography was almost flat and the water content of ice (which affects to propagation speed) was almost constant. Figure 5 shows that the 800-MHz GPR has a potential to identify the subglacial reflection from 15 m depth in temperate glaciers. On the other hand, if ice thickness (d) is smaller than about 2 m, it is difficult to separate it from the air wave. Besides the subglacial reflection, several englacial reflections were also found. For example, we can see a convex-shape reflection at the distance of 22 m nearby the bedrock. It is probably due to water-induced open cavity or subglacial crevasses.

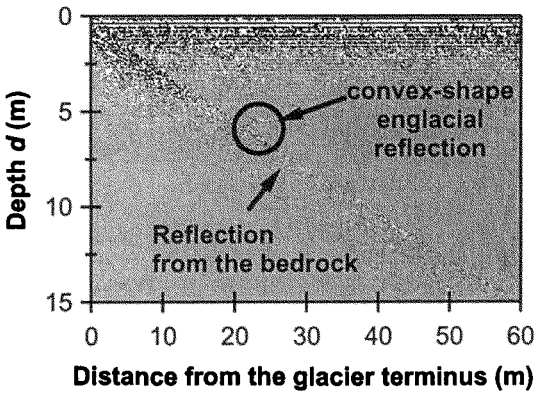

Fig. 5. Pseudo-cross section of the glacier terminus obtained with GPR. Stronger and smaller received signals represent with darker and lighter colors. A continuous echo between the left top and the right bottom is from the subglacial interface. The circle shows the location of a convex-shape englacial reflection.

Gades *et al.* (2000) showed that a one-half sum-of-squared voltage amplitude (V) within a given time window is a proxy of reflection power. Then, V for subglacial reflections (Vs) is useful to investigate subglacial conditions (Copland and Sharp, 2001; Gades *et al.*, 2000). We calculated Vs with the same manner, when $d>2$ m (Fig. 6). Since period of 800-MHz radio

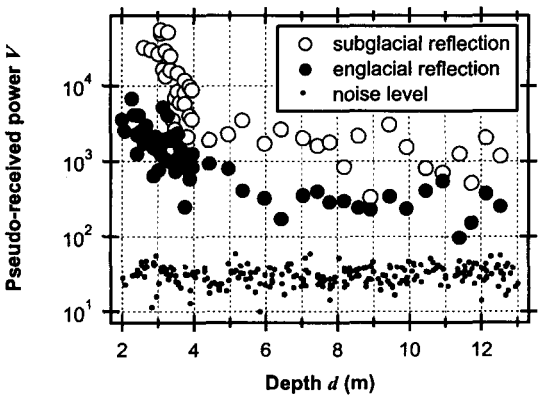

Fig. 6. Proxy of received power from englacial and subglacial reflectors (*Ve* and *Vs*). Proxy of noise level (*Vi*) is also shown. Just for convenience, *Ve* and *Vs* are biased -10,000 and +10,000 digits, respectively. *Ve* and *Vs* for $d>4$ m were sampled at an interval of 10 data (approximately, 0.5 m).

wave is 1.25 ns in ice, we choose the time window as 12 ns. Variations of *Vs* are caused by changes of ice thickness, basal characteristics, englacial structures and noise level of the instruments. To separate these effects and to know the basal characteristics, we also calculated *V* for englacial reflections (*Ve*) and for noise level (*Vn*), which are also shown in Fig. 6. *Vs* is inversely proportional to the ice thickness in the range of $2<d<5$ m. Moreover, since smaller *Vs* can be caused by larger *Ve*, *Vs* and *Ve* has rough anti-phase correlation in the range of $d>4$ m. However, for instance, *Ve* decreases with depth for $d<4$ m, where *Ve* also decreases. Then, features in *V* are much more complex than the previous study. Possible causes of this discrepancy are radar frequency and water existence within the ice. We observed a temperate glacier at 800 MHz. Instead, Gades *et al.* (2000) investigated cold ice at several megahertz. Since we observe back scattering from targets, we can not detect defuse reflection components. However, if frequency is high, the components are relatively significant. Moreover, if water exists not as layers but as separately, the water may cause large defuse scattering components. Then, we can not evaluate *V* simply with depth and/or anti-phase relation between *Ve* and *Vs*. This requires more detail studies to apply the method to high-frequency radar surveys in temperate glaciers.

4.2.3. Debris thickness on the ice-cored moraine

Results of GPR surveys along the lines A and B are shown in Fig. 7. Since we confirmed with pit

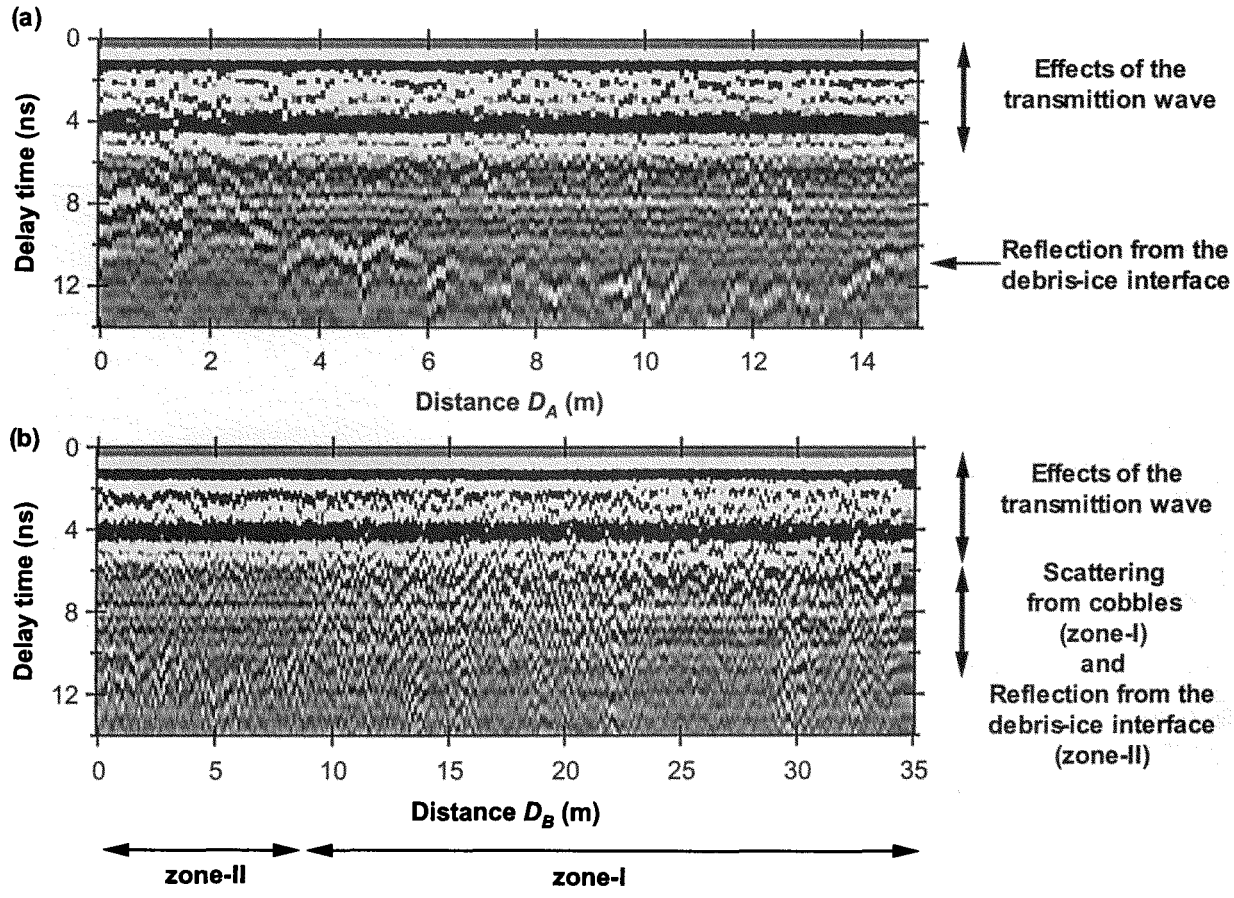

Fig. 7. Pseudo-cross section of ice-cored moraine along the line A (a) and line B (b). Signal changes for the delay time <4 ns are affected by the transmission wave. Continuous reflections in the panel a and zone-II in the panel b are from the ice/debris interface.

works that there are no clear boundary within the debris at $D_A = D_B = 6$ m, we concluded that the continuous clear reflection was from the debris/ice interface. The reflection from the debris/ice interface was clearly obtained along the line A, whereas it was obtained only for $0 < D_B <$ around 8 m along the line B. Zone-I and -II in the panel b (shown at the bottom) indicate that there are cobble at the top of debris or not, respectively. As shown in Fig. 2, there were cobbles at the top of the debris for zone-I. The location of debris-components transition is coincident with boundary where we can identify reflection from the debris/ice interface or not. The GPR detected the scattered radio wave from within the antenna aperture. Since the effective antenna aperture of the GPR was around 45° (Yamamoto, 2002), we can consider that scattering from the cobbles within the antenna aperture masked the reflection from the interface.

Propagation speed of radio wave is not known for such complex materials as debris. Comparison between d (42 cm) and the delay time (10.2 ns) at the site of $D_A = D_B =$ 6 m gave the propagation speed as 82 m μs^{-1}. This speed is equivalent to the permittivity of 13. Evaluation of this large permittivity with the pit-observation data is a future subject.

5. Summary

We performed field tests of a novel ice-penetrating radar (IPR) and commercial ground-penetrating radar (GPR) in Athabasca Glacier, Jasper National Park, Alberta, Canada in September, 2001. Both instruments worked well under severe conditions in general. Performance of the IPR did not check sufficiently, but the IPR measured about 100-m ice thickness. GPR was also measured up to 15 m ice thickness at the glacier terminus. Moreover, the GPR observed continuous interface between ice and debris within ice-cored moraine. However, more detailed studies are required to evaluate received power quantitatively.

Acknowledgments

We could not carry out short-term efficient operations without kind supports of Parks Canada and Brewster Company. Special thanks are due to Matty Gibson (supervisor of the icefield center), Ed Newport (operation manager of snocoach), and their stuff. The novel glacier profiler system with the portable low-frequency ice-penetrating radar was developed through a cooperative study with Walnut Company, Tachikawa, Japan, for which we are grateful to Ryoji Saito. We also thank Garry Clarke of University of British Columbia, Michael Demuth of Geological Survey of Canada, and Charlie Raymond of University of Washington for their valuable suggestions to this field work. This study is partly supported by a Grant-in-Aid for Scientific Research (B, 2, No. 12554015) of the Ministry of Education, Culture, Sports, Science and Technology of Japan.

References

Bogorodskiy, V. V., Bentley, C. R., and Gudmandsen, P. E. (1985): *Radioglaciology*. D. Reidel.

Copland, L., and Sharp, M. (2001): Mapping thermal and hydrological conditions beneath a polythermal glacier with radio-echo sounding. J. Glaciol. **47**, 232-242.

Fujita, S., Matsuoka, T., Ishida, T., Matsuoka, K., and Mae, S. (2000): A summary of the complex dielectric permittivity of ice in the megahertz range and its application for radar sounding of polar ice sheets. In *Physics of Ice Core Records*. (T. Hondoh, Ed.), pp. 185-212, Sapporo.

Gades, A. M., Raymond, C. F., Conway, H., and Jacobel, R. W. (2000): Bed properties of Siple Dome and adjacent ice streams, West Antarctica, inferred from radio-echo sounding measurements. J. Glaciol. **46**, 88-94.

IAHS/UNESCO. (1998): *Fluctuations of glaciers 1990-1995*. World Glacier Monitoring Service, Zurich.

Macheret, Y. Y., Moskalevsky, M. Y., and Vasilenko, E. V. (1993): Velocity of radio-waves in glaciers as an indicator of their hydrothermal state, structure and regime. J. Glaciol. **39**, 373-384.

Meier, M. F. (1984): Contribution of Small Glaciers to Global Sea-Level. Science **226**, 1418-1421.

Moore, J. C., PaDoalli, A., Ludwig, F., Blatter, H., Jania, J., Gadek, B., Glowacki, P., Mochnacki, D., and Isaksson, E. (1999): High-resolution hydrothermal structure of Hansbreen, Spitsbergen, mapped by ground-penetrating radar. J. Glaciol. **45**, 524-532.

Paren, J. G., and Robin, G. de Q. (1975): Internal reflections in polar ice sheets. J. Glaciol. **14**, 251-259.

Plewes, A. L., and Hubbard, B. (2001): A review of the use of radio-echo sounding in glaciology. Prog. Phys. Geogr. **25**, 203-236.

Reynolds, J. R., and Young, G. J. (1997): Changes in areal extent, elevation and volume of Athabasca Glacier, Alberta, Canada, as estimated from a series of maps produced between 1919 and 1979. Ann. Glaciol. **24**, 60-65.

Rutter, N. W., and Luckman, B. (1987): Athabasca Glacier. In Twelveth INQUA congress field excursion C-16. (J. Dormaar, L. V. Hills, B. Luckman, G. Osborn, B. O. K. Reeves, N. W. Rutter, M. C. Wilson, and N. R. Catto, Eds.), pp. 54. National Research Council, Canada, Ottawa.

Trombley, T. J. (1986): A radio echo-sounding survey of Athabasca Glacier, Alberta, Canada. Unpublished Master thesis, University of New Hampshire.

Yamamoto, T. (2002): Observation of internal structures of snowcovers with a ground-penetrating radar. unpublished Master thesis, Hokkaido University. (in Japanese)